PHYSICAL REVIEW B **84**, 140510(R) (2011)

Non-Gaussian self-dynamics of liquid hydrogen

Milva Celli,[1] Ubaldo Bafile,[1] Daniele Colognesi,[1] Alessio De Francesco,[2] Ferdinando Formisano,[2] Eleonora Guarini,[3] Martin Neumann,[4] and Marco Zoppi[1]

[1]*Consiglio Nazionale delle Ricerche, Istituto dei Sistemi Complessi, via Madonna del Piano 10, I-50019 Sesto Fiorentino, Italy*

[2]*Consiglio Nazionale delle Ricerche, Istituto Officina dei Materiali, Operative Group in Grenoble (OGG), c/o Institut Laue-Langevin, 6 rue J. Horowitz, Bôite Postal 156, F-38042, Grenoble Cedex 9, France*

[3]*Dipartimento di Fisica e Astronomia, Università di Firenze, via G. Sansone 1, I-50019 Sesto Fiorentino, Italy*

[4]*Fakultät für Physik der Universität Wien, Strudlhofgasse 4, A-1090 Wien, Austria*

(Received 2 June 2011; revised manuscript received 27 September 2011; published 31 October 2011)

The Gaussian approximation (GA) is widely employed in the description of single-molecule dynamics in liquids. In the GA framework it is assumed that the motion of particles is only determined by the time autocorrelation function of the particle velocity, in the whole wave-vector Q range of time- and space-dependent diffusive dynamics. Although often adopted, the validity of GA is not yet well assessed in different Q ranges, especially for the so-called quantum Boltzmann fluids. Liquid hydrogen, the most relevant test case for quantum dynamics simulation techniques, is also the canonical choice for experiments in self-dynamics, thanks to its ideal suitability to inelastic incoherent neutron scattering studies. Experimental evidence of the GA breakdown in hydrogen was recently achieved, but, to the best of our knowledge, the localization in Q space of non-Gaussian behavior was still undetermined, and no quantitative assessment has been obtained yet. These issues have been tackled and solved by a recent neutron investigation in conjunction with a quantum simulation of the velocity autocorrelation function.

DOI: 10.1103/PhysRevB.84.140510 PACS number(s): 67.63.Cd, 66.10.cg, 78.70.Nx

Understanding the single-particle, or *self*-, dynamics of liquids is a longstanding research theme in condensed-matter physics.[1,2] One of the most important approaches to this problem is based on the so-called Gaussian approximation (GA),[3] which owes its name to the assumption that the self-intermediate scattering function is given by

$$F_s(Q,t) = \exp[-Q^2 w(t)]. \tag{1}$$

According to the standard definition[4] for an isotropic system of N identical particles, $F_s(Q,t) = (\frac{1}{N})\sum_{j=1}^{N}\langle \exp[-i\mathbf{Q}\cdot\mathbf{r}_j(0)]\exp[i\mathbf{Q}\cdot\mathbf{r}_j(t)]\rangle$ is the time autocorrelation of the spatial Fourier components, with wave vector $\mathbf{Q}$, of the microscopic density fluctuations, $\mathbf{r}_j(t)$ is the Heisenberg position operator for the jth particle at time t, $\langle\cdots\rangle$ indicates a quantum statistical average, and $Q = |\mathbf{Q}|$. Equation (1) states that in the whole dynamical range between hydrodynamic diffusion ($Q \to 0$ and long times) and free-particle motion ($Q \to \infty$ and short times) there exists a function of time only $w(t)$ that completely determines the motion of a particle. The GA finds its rationale in the fact that in a fluid Eq. (1) is valid in both the above limit conditions, so that large deviations from GA should not be reasonably expected at the nanometer-picosecond length and time scales relevant to molecular motions. Equation (1) is also exact for an isotropic harmonic crystal.

Rahman *et al.*[5] have shown that in an isotropic system one can rigorously write

$$F_s(Q,t) = \exp\left[\sum_{p=1}^{\infty}(iQ)^{2p}\gamma_p(t)\right]. \tag{2}$$

Here

$$\gamma_1(t) = -i\frac{\hbar t}{2M} + \frac{1}{3}\int_0^t dt_1(t-t_1)u(t_1), \tag{3}$$

where $u(t) = \langle \mathbf{v}(0)\cdot\mathbf{v}(t)\rangle$ is the velocity autocorrelation function (VACF), $\mathbf{v}(t)$ is the velocity of any tagged particle in the fluid, and Eq. (3) also includes the free-recoil effect for particles of mass M ($\hbar$ is the Planck constant). The GA is obtained from the simple neglect of all $\gamma_p(t)$ with $p > 1$, the self-dynamics being then derivable from knowledge of $u(t)$ alone, through the use of its power spectrum $f(\omega)$ defined below.[5]

The non-GA terms in the expansion (2) contain functions $\gamma_p(t)$ expressed as multiple integrals of correlation functions of increasing order which involve the velocity of a tagged particle at various points in time. While GA assumes that higher-order correlations can be factored as the product of two-time velocity correlation functions evaluated at different instants, the non-GA behavior is bound to the presence of irreducible many-velocity correlations. Rigorous definitions of the $\gamma_p(t)$ are given in Ref. 5, although the treatment is rather formal. A more intuitive insight may be gained by noting that, in the high-Q regime, the Gaussian behavior stems from the assumptions of a Maxwell equilibrium distribution of velocities and of uncorrelated binary collisions. Non-Gaussianity may then set on with decreasing Q due to the role played by sequences of collisions where the particle velocities are not statistically independent. Another clue is also provided by the remark[1] that non-Gaussian dynamics is associated with spatial correlations in the fluid described by higher-order moments of the Van Hove self-correlation function $G_s(r,t)$, i.e., the real-space transform of $F_s(Q,t)$, leading to the concept of a generalized, effective space-dependent diffusion constant.

The VACF is best, and usually, determined from computer simulations. Molecular dynamics (MD) computations have been able to reproduce to an ever-growing degree the behavior of classical fluids, in comparison to theory as well as experiments.[6] On the other hand, the accurate description of the dynamics remains an open problem for the so-called

quantum Boltzmann liquids (QBLs),[7] which feature relevant quantum delocalization effects but can still be thought of as consisting of distinguishable particles obeying Boltzmann statistics. Molecular hydrogen, which at the temperature of the liquid state is found in its *para* species where the molecules have zero nuclear spin and populate the $J = 0$ rotational level only, is the prototypical and most studied QBL. In fact, apart from the obvious interest in the system itself, liquid para-H_2 has become a standard benchmark[8] for the development of QBL dynamics simulation techniques, a subject to which much effort has been devoted in recent years.[8–10] Also, hydrogen is by far the best sample for such experimental studies due to its very large cross section for incoherent neutron scattering, which is the most important probe of the self-dynamics in the microscopic (Q,ω) range of interest.

To the best of our knowledge, a critical assessment of GA is still lacking. Although neutron scattering[11] and MD simulations[12] on classical fluid argon have shown that regions of the (Q,ω) plane exist, where GA is not rigorously valid, that approximation was widely used as a working hypothesis, especially in QBL studies,[7,13] despite its need of an experimental validation or rebuttal.

In the case of H_2, neutron scattering provided an important result a few years ago,[14] although the data were not obtained as constant-Q spectra. Without resorting to a quantum-simulated VACF, the center-of-mass self-dynamic structure factor $S_s(Q,\omega) = \frac{1}{2\pi}\int_{-\infty}^{\infty} dt\, \exp(-i\omega t) F_s(Q,t)$ was computed within GA with an adjustable model of $f(\omega)$, fitted to reproduce the neutron spectrum in a Q range $\sim$20 nm^{-1}. This $f(\omega)$ was then used, again within GA, to compute the spectrum in a higher-Q range ($\sim$40 nm^{-1}), where a clear discrepancy appeared with respect to the measurements. The breakdown of GA in liquid para-H_2 was then inferred, since it turned out to be impossible to find a unique Q-independent $f(\omega)$ reproducing the experimental data in both investigated regions of Q. Nevertheless, the question whether $S_s(Q,\omega)$ can actually be derived, at specific Q values, using the GA with the *true* but unknown VACF, remained unanswered. In particular, while at first sight the above result might suggest a loss of validity of GA with increasing Q, at least in the range explored, this may well be too simple a conclusion, as indeed reported below. The works in Ref. 14 pointed out the need for a wider exploration of the (Q,ω) plane at constant-Q conditions. This prompted us to perform a new neutron study accompanied by a quantum simulation of the VACF performed with the path integral centroid molecular dynamics (PICMD) algorithm.[9] Here we report on the results of this investigation as far as the validity of GA is concerned.

The inelastic scattering of neutrons from a liquid para-H_2 sample, at temperature $T = 15.7$ K and a molecular number density of 22.53 nm^{-3},[15] was recorded with two time-of-flight spectrometers at the Institut Laue-Langevin (ILL, Grenoble, France). The small-angle setup of the Brillouin spectrometer (BRISP) with an incident neutron energy $E_0 = 50$ meV was used for Q values not exceeding 10 nm^{-1}, while for $20 \leqslant Q/\text{nm}^{-1} \leqslant 45$ the experiment was carried out on the IN4C spectrometer ($E_0 = 65.2$ meV).

Neutron spectra of fluid hydrogen are well described by the Young-Koppel model[16] based on the fact that H_2 molecules can be treated as vibrating free rotors even in the condensed phases.[17] Neglecting the very small coherent scattering, and taking into account the population of rotational levels and the fact that no transitions from the vibrational ground state are permitted by the available neutron energy, the double-differential cross section is made of replicas of $S_s(Q,\omega)$ shifted by the rotational energies of the $J = 0 \rightarrow$ odd transitions.[18] Due to the light molecular weight, these lines are well separated and only the most intense of them, the $J = 0 \rightarrow 1$ transition corresponding to a shift $\hbar\omega_{0\rightarrow 1} = 14.69$ meV, is probed in the energy window of the experiment. The double-differential cross section is then

$$\frac{d^2\sigma}{d\Omega\, d\omega} = \frac{k'}{k} a(Q)_{0\rightarrow 1} S_s(Q,\omega - \omega_{0\rightarrow 1}), \tag{4}$$

where k and k' are the neutron wave vectors before and after scattering. $a(Q)$ is a known, transition-specific form factor given in this case by[19]

$$a(Q)_{0\rightarrow 1} = 3b_{\text{inc}}^2 \left| \int_{-1}^{1} dx\, x \exp(-\alpha^2 x^2/2) \sin(\eta x) \right|^2, \tag{5}$$

where b_{inc} is the bound incoherent scattering length of the hydrogen nucleus and the integral can be evaluated numerically with $\eta = Qr_e/2$ and $\alpha^2 = \frac{\hbar Q^2}{4M\omega_v}$. Here, r_e is the equilibrium distance between the H atoms in the molecule and ω_v is the vibrational quantum.

Through Eq. (4), a constant-Q experimental $S_s(Q,\omega)$ was obtained to within a normalization factor, although the result was still broadened by a resolution function $R(\omega)$, measured from the scattering of a vanadium sample to be a Gaussian with a half width at half maximum (HWHM) of 0.55 and 1.39 meV for BRISP and IN4C, respectively.

Despite their importance and partial successes, PICMD and similar methods (e.g., ring polymer molecular dynamics) do not capture the full quantum character of a many-body molecular system, as far as exchange effects and treatment of quantized rotations are concerned. Fortunately, in the case of liquid para-H_2, these deficiencies have no consequences, since quantum exchange was shown to be irrelevant,[20] and quantum rotations are actually factored out of our calculation, as already discussed. Indeed, almost all published quantum simulation results on liquid para-hydrogen, based on such assumptions, provide results in quite satisfactory agreement with the experimental measurements of mean kinetic energy, diffusion coefficient, and structural properties.

The PICMD method was applied to a system of 256 molecules interacting via the Silvera-Goldman potential.[21] The Trotter number, i.e., the number of beads on the classical ring polymers replacing the quantum mechanical particles, was 64. In contrast to the usual implementation, the calculation of the quantum mechanical forces, which are required at each time step of the otherwise classical simulation, was performed by the path integral Monte Carlo method, rather than MD, thus avoiding sampling problems associated with the stiff "intramolecular" modes of the polymers and allowing for a much larger time step. The simulation was extended up to 1 ns in the isokinetic ensemble, ensuring thermal stability and statistically very reliable data. The velocity correlation was

calculated up to a maximum time lag of 1.5 ps. A shorter test run with 500 particles confirmed that the shape of the VACF was not noticeably influenced by finite-size effects. The output of a PICMD simulation is the *canonical* (or Kubo-transformed[22]) VACF

$$u_c(t) = \frac{1}{\beta}\int_0^\beta d\lambda \langle e^{\lambda\mathcal{H}}\mathbf{v}(0)\cdot e^{-\lambda\mathcal{H}}\mathbf{v}(t)\rangle, \tag{6}$$

where $\beta = 1/(k_B T)$, k_B is the Boltzmann constant, $\mathbf{v}(t)$ is the center-of-mass velocity, and $\mathcal{H}$ is the Hamiltonian operator of the system. From $u_c(t)$, the spectral function

$$f(\omega) = \frac{M\beta}{3\pi}\int_{-\infty}^{\infty} dt\, e^{-i\omega t}u_c(t) \tag{7}$$

was then obtained, and the GA expression for the intermediate scattering function[5]

$$F_s(Q,t) = \exp\left\{-\frac{\hbar Q^2}{2M}\int_0^\infty d\omega \frac{f(\omega)}{\omega} \times\left[[1-\cos(\omega t)]\coth\left(\frac{\beta\hbar\omega}{2}\right) - i\sin(\omega t)\right]\right\}, \tag{8}$$

calculated at the experimental Q values, was finally Fourier transformed and convoluted with $R(\omega)$. The resulting spectra were compared with the experimental ones normalized by a factor determined at the highest Q values, where they turned out to have the same shape as the computed ones (see below). Also, we made allowance for the presence in the data of a possible residual background, to be subtracted in the form of a low-degree polynomial function of frequency, in much the same way as done in Ref. 14. A linear function of ω, with coefficients only weakly dependent on Q, was found to be sufficient. These results make us confident that, while eliminating minor spurious effects, no significant distortion of the system response was introduced. Figure 1 shows the measured and the GA-computed spectra for one Q value in the BRISP range and five values in the IN4C case.

As far as the low-Q data are concerned, the agreement is good, and the validity of GA in this range can be confirmed. This statement has to be taken with caution, however, since the resolution broadening strongly affects the shape of an intrinsically narrow line. On the other hand, assuming that GA produces an $S_s(Q,\omega)$ really different from the true one would then require to admit that the resolution broadening is such as to exactly mask the non-Gaussian contributions, a result which seems a rather unlikely coincidence.

With the IN4C data, we find substantial agreement at the highest Q, while an increasing discrepancy emerges with decreasing Q. The deficiencies of GA are thus evident, but we now obtain as further results that (a) non-Gaussian effects in $F_s(Q,t)$ practically vanish at Q below 10 nm^{-1} and again at ~40 nm^{-1} and above; (b) the maximum deviation from GA is located somewhere between 10 and 20 nm^{-1}, where its detection is, unfortunately, severely hampered by intrinsic resolution limitations. In fact, the lower frames of Fig. 1 show that this deviation gradually decreases by increasing Q above 20 nm^{-1}.

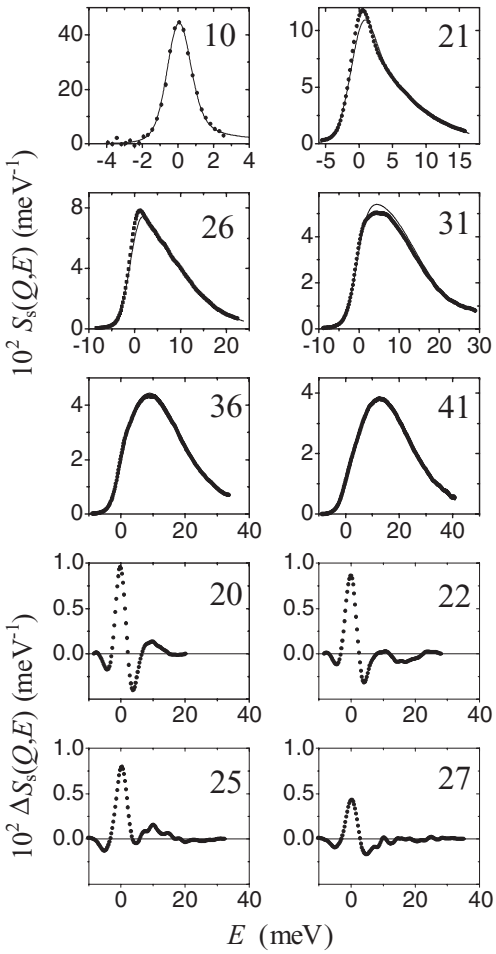

FIG. 1. The top six frames show the self-dynamic structure factor obtained from neutron data (dots) and within GA calculated with the quantum simulated VACF (line). The number in the top right-hand corner of each frame is the Q value in units of nm^{-1}. In the top left-hand frame the neutron data are from the BRISP experiment, and in the five other frames from the IN4C experiment. All the spectra are broadened by the instrumental resolution. The peak position shifts to the right-hand side with increasing Q due to the molecular recoil. The bottom four frames display the difference between experimental and calculated data, at four additional Q values.

We restrict ourselves to using IN4C data in order to extract the maximum information available about non-Gaussianity. We write the Fourier transform from ω to t space of the resolution-broadened experimental spectra in the form

$$\tilde{F}(Q,t) = R(t)F_s(Q,t) = R(t)e^{-Q^2[A'(Q,t)+iA''(Q,t)]}, \tag{9}$$

where the prime and double prime denote the real and imaginary parts of complex quantities, $R(t)$ is the Fourier transform of $R(\omega)$, and

$$A(Q,t) = \gamma_1(t) - Q^2\gamma_2(t) + Q^4 x(t). \tag{10}$$

$x(t)$ is meant to be a remainder including all possible contributions beyond the Q^2 term and modeled, somewhat roughly, in the simplest possible way, as we make here the assumption that most of the non-Gaussian dynamical

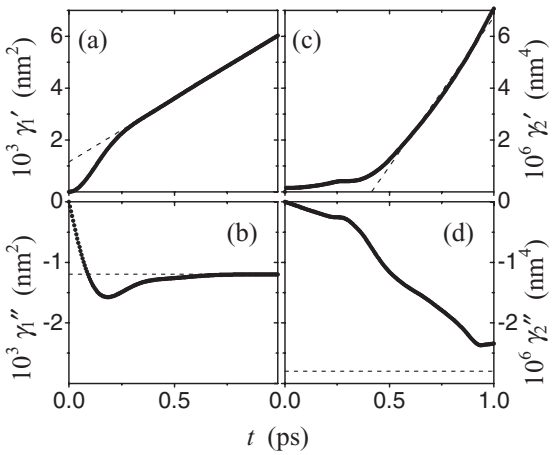

FIG. 2. Short-time behavior of the real (a) and imaginary (b) parts of $\gamma_1(t)$ as calculated by PICMD, and of the real (c) and imaginary (d) parts of the first non-Gaussian term $\gamma_2(t)$ as derived through the procedure described in the text. In the top frames, the dashed line shows the large-time linear behavior, determined as a straight line fitted to the data in the time interval between 0.6 and 1.0 ps. In the bottom frames the large-time limit is calculated from $\gamma_p''(t) \approx -(\hbar\beta/2)D_p$, where D_p is the real-part asymptotic slope.

behavior is accounted for by $\gamma_2(t)$ and no attempt is made at characterizing higher-order corrections. At each t, with $\gamma_1'(t)$ and $\gamma_1''(t)$ fixed to their PICMD values, parabolic fits of A' and A'' as functions of Q^2 provide $\gamma_2'(t)$ and $\gamma_2''(t)$ as initial-slope coefficients, as displayed in Fig. 2.

We first observe that $\gamma_2(t)$ is nearly three orders of magnitude smaller than $\gamma_1(t)$, while the remainder $x(t)$ (not shown) is of the order of 10^6 times smaller, supporting the assumption that its contribution is fully negligible.

Second, we note that $\gamma_2(t)$ can only be studied at short times. This is due to the fact that, in order to obtain A' and A'', one has to divide $\tilde{F}(Q,t)$ by $R(t)$, that is a Gaussian function with a HWHM of ∼0.6 ps. At times larger than ∼1 ps the fast decrease of the $R(t)$ tails produce meaningless data since the main effect of the division becomes noise amplification. At present, this appears to be an intrinsic limitation, due to the lack of instruments able to better resolve a spectral line located at ∼15 meV, thus requiring for its excitation a neutron energy of tens of meV. Nevertheless, at $t = 1$ ps, $\gamma_2'(t)$ seems to have already approached an asymptotic linear behavior as predicted by theory, with $\gamma_p'(t) \approx D_p t - C_p'$ at large times.[5] The same, in fact, happens with $\gamma_1'(t)$, which has the expected slope given by the self-diffusion coefficient $D = D_1$. As for the imaginary part, known to tend to the large-time-limit negative constant value $\gamma_p''(t) \approx -C_p'' = -(\hbar\beta/2)D_p$,[5] the asymptotic regime is attained by $\gamma_1''(t)$ at $t \sim 1$ ps. Besides the resolution limitation, the extraction of $A''(Q,t)$ as the argument of an oscillatory function (a complex exponential) is a further difficulty, and we can only obtain $\gamma_2''(t)$ as a semiquantitative estimate, which, however, shows the correct order of magnitude and seems to approach the expected asymptote in the explorable time range.

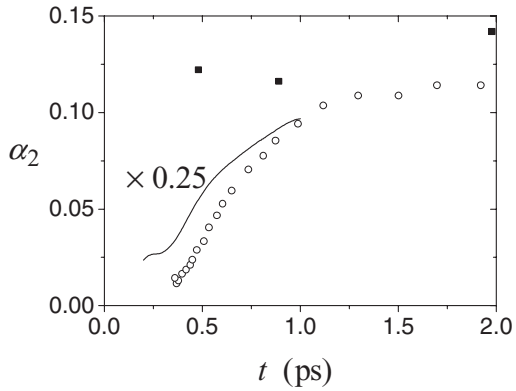

FIG. 3. Non-Gaussianity parameter $\alpha_2(t)$ in argon and para-H_2. The argon data are read off from Fig. 14 of Ref. 11, which shows the authors' experimental data and the simulation results by Levesque and Verlet quoted therein. These data are displayed here as black squares and circles, respectively. The present para-hydrogen result (solid line), reduced by a factor of 4 to allow for an easier comparison, refers to the real part of $\alpha_2(t)$, which also has a much smaller imaginary component.

The expansion in Eq. (2) can also be written in the equivalent form[1]

$$F_s(Q,t) = e^{-Q^2\gamma_1(t)}\{1 + [Q^2\gamma_1(t)]^2\alpha_2(t)/2 - \cdots\}, \quad (11)$$

where the first non-Gaussian term is expressed by the function $\alpha_2(t) = 2\gamma_2(t)/\gamma_1^2(t)$. An estimate of this quantity can be obtained from our determination of the first two γ's, at least at times not so close to zero as to suffer from the numerical problems related to taking the ratio of vanishing quantities. In Fig. 3 we compare our results for para-H_2 with those reported in Ref. 11 for argon, expressed in terms of $\alpha_2(t)$. The hydrogen data are limited to the real part of $\alpha_2(t)$ and, for ease of comparison, have been divided by a factor of 4. In the time range where data on both fluids are available, the results appear to be qualitatively similar, but the effect of the first non-Gaussian correction is clearly larger in H_2.

Summarizing, a careful neutron study of the self-dynamics of liquid para-hydrogen has not only confirmed the presence of non-Gaussian dynamics, but also provided knowledge about the specific Q range in which the experimental data cannot be properly analyzed within the framework of the GA. The comparison with GA spectra computed from the PICMD-simulated VACF reveals non-Gaussian behavior below $Q \sim 40$ nm^{-1} and a smooth approach to the expected high-Q recovery of Gaussian dynamics. On the other hand, detecting where exactly the onset of non-Gaussianity starts in the low-Q regime remains far more demanding, since the narrower the spectra the severer the resolution limitations of available neutron spectrometers. This work has also provided a determination of non-Gaussian effects in the $\gamma_p(t)$ expansion of Eq. (2) for a quantum liquid in the important subpicosecond regime.

The Scientific Membership Agreement between Consiglio Nazionale delle Ricerche and ILL and the skillful technical assistance of ILL staff are gratefully acknowledged.

[1]J. P. Boon and S. Yip, *Molecular Hydrodynamics* (McGraw-Hill, New York, 1980).
[2]U. Balucani and M. Zoppi, *Dynamics of the Liquid State* (Clarendon, Oxford, 1994).
[3]G. H. Vineyard, Phys. Rev. **110**, 999 (1958).
[4]L. Van Hove, Phys. Rev. **95**, 249 (1954).
[5]A. Rahman, K. S. Singwi, and A. Sjölander, Phys. Rev. **126**, 986 (1962).
[6]M. P. Allen and D. J. Tildesley, *Computer Simulation of Liquids* (Oxford University Press, Oxford, UK, 1987).
[7]J. Cao and G. A. Voth, J. Chem. Phys. **100**, 5106 (1994); G. J. Martyna, *ibid.* **104**, 2018 (1996); E. Rabani and D. R. Reichman, *ibid.* **116**, 6271 (2002); D. R. Reichman and E. Rabani, *ibid.* **116**, 6279 (2002).
[8]J. Cao and G. J. Martyna, J. Chem. Phys. **104**, 2028 (1996); M. Zoppi, D. Colognesi, and M. Celli, Europhys. Lett. **53**, 34 (2001); M. Celli, D. Colognesi, and M. Zoppi, J. Low Temp. Phys. **126**, 585 (2002); I. R. Craig and D. Manolopoulos, J. Chem. Phys. **121**, 3368 (2004); J. Liu and W. H. Miller, *ibid.* **128**, 144511 (2008).
[9]A. Calhoun, M. Pavese, and G. A. Voth, Chem. Phys. Lett. **262**, 415 (1996); M. Pavese and G. A. Voth, Chem. Phys. Lett. **249**, 231 (1996); K. Kinugawa, *ibid.* **292**, 454 (1998); Y. Yonetani and K. Kinugawa, J. Chem. Phys. **119**, 9651 (2003); T. D. Hone and G. A. Voth, *ibid.* **121**, 6412 (2004).
[10]J. Cao and G. A. Voth, J. Chem. Phys. **101**, 6168 (1994); N. Makri, Annu. Rev. Phys. Chem. **50**, 167 (1999).
[11]K. Sköld, J. M. Rowe, G. Ostrowski, and P. D. Randolph, Phys. Rev. A **6**, 1107 (1972).
[12]R. C. Desai, J. Chem. Phys. **44**, 77 (1966); T. Tsang, Phys. Rev. A **17**, 393 (1978).
[13]M. Celli, D. Colognesi, and M. Zoppi, Phys. Rev. E **66**, 021202 (2002); E. Rabani and D. R. Reichman, *ibid.* **65**, 36111 (2002).
[14]D. Colognesi, M. Celli, M. Neumann, and M. Zoppi, Phys. Rev. E **70**, 061202 (2004); M. Celli, D. Colognesi, A. J. Ramirez-Cuesta, and M. Zoppi, Physica B **350**, e1083 (2004).
[15]H. M. Roder, G. E. Childs, R. D. McCarty, and P. E. Angerhofer, NBS Technical Note No. 641, 1973.
[16]J. A. Young and J. U. Koppel, Phys. Rev. A **135**, 603 (1964).
[17]J. Van Kranendonk, *Solid Hydrogen* (Plenum, New York, 1983).
[18]K. P. Huber and G. Herzberg, *Constants of Diatomic Molecules* (Van Nostrand, New York, 1979).
[19]E. Guarini, J. Phys. Condens. Matter **15**, R775 (2003).
[20]M. Boninsegni, Phys. Rev. B **79**, 174203 (2009).
[21]I. F. Silvera and V. V. Goldman, J. Chem. Phys. **69**, 4209 (1978).
[22]R. Kubo, Rep. Prog. Phys. **29**, 255 (1966).